ORIGINAL RESEARCH ARTICLE

In Vitro Regional Deposition of Nasal Sprays in an Idealized Nasal Inlet: Comparison with *In Vivo* Gamma Scintigraphy

John Z. Chen[1] · Warren H. Finlay[1] · Andrew Martin[1]

Abstract

Purpose To compare *in vitro* regional nasal deposition measurements using an idealized nasal airway geometry, the Alberta Idealized Nasal Inlet (AINI), with *in vivo* regional deposition for nasal drug products.

Materials and Methods One aqueous solution formulation (NasalCrom), one aqueous suspension formulation (Nasonex) and one nasal pressurized metered dose spray device (QNASL) were selected. Two spray orientation angles, 60° and 45° from the horizontal, were selected. A steady inhalation flow rate of 7.5 L/min was selected to simulate slow inhalation through a single nostril. After actuation, the AINI was disassembled. The mass of drug deposited in each region and a downstream filter, representing penetration of drug to the lungs, was determined using ultraviolet–visible (UV–Vis) spectrophotometry.

Results No filter (lung) deposition was detected for NasalCrom or Nasonex. Filter deposition ranged from 6 to 11% for QNASL. For NasalCrom, 45% to 69% of the dose deposited in the AINI was deposited in the vestibule and 31% to 55% was deposited in the turbinates; for Nasonex, 66% to 74% (vestibule) and 26% to 34% (turbinates); for QNASL, 90% to 100% (vestibule) and 0% to 10% (turbinates). No statistically significant difference was observed between regional deposition *in vivo* and *in vitro* for any of the formulations, except that nasopharyngeal deposition with Nasonex differed by less than 1.56% from *in vivo*, which while statistically significant, is unlikely to be clinically significant.

Conclusions The AINI was able to mimic regional *in vivo* deposition for nasal drug products, permitting differentiation between devices based on regional deposition.

Keywords aerosols · *in vitro-in vivo* correlations · nasal sprays · regional deposition

Introduction

Benchtop *in vitro* test methods are vital to researchers and drug developers seeking to understand or characterize the performance of medical aerosols and nasal sprays. For example, the United States Pharmacopeia General Chapter < 601 > contains standardized *in vitro* procedures for the measurement of properties of medical aerosol and nasal spray products, such as delivered dose uniformity, aerodynamic size distribution and fine particle fraction, that facilitate comparisons between different products and give some indication of the possible behavior of the product *in vivo* [1]. For nasal spray drug products, FDA guidance recommends additional *in vitro* tests, including characterization of spray pattern and plume geometry [2]. Knowledge of the spray characteristics of a test formulation can be particularly valuable in the early stages of product development, where parameter refinement based on early feedback from *in vitro* experiments can save time later in the development process when testing moves to an *in vivo* setting. Measured *in vitro* parameters are also intended to provide a convenient way to support assessment of bioavailability and bioequivalence of different nasal spray products, and should ideally be highly discriminating between products [2–4]. However, the strength of correlation between *in vitro* measurement parameters for nasal spray products and relevant *in vivo* responses remains uncertain and is a topic of frequent debate.

In the related field of aerosol drug delivery to the lungs, researchers have described *in vitro* methods using idealized or selected realistic airway geometries that mimic average deposition measured in *in vivo* studies [5–13]. These geometries can function as a reference for *in vitro* experiments

✉ Andrew Martin
andrew.martin@ualberta.ca

1 Department of Mechanical Engineering, Faculty
of Engineering, University of Alberta, 10-265 Donadeo
Innovation Centre for Engineering, Edmonton, Canada

or *in silico* simulations, facilitating prediction of *in vivo* performance at early stages of drug or device development, and allowing comparable results to be obtained between laboratories.

For nasal drug delivery, a representative geometry mimicking average *in vivo* regional spray deposition across a wide parameter space has not been definitively established, despite significant past research effort [14–17]. Recently, a new geometry was proposed based on extensive computational fluid dynamics (CFD) simulations performed in a set of realistic nasal geometries [18]. In a subsequent publication, Chen *et al.* (2020) designed and executed an *in vitro* study to validate the performance of the idealized geometry, fabricated in plastic using stereolithography, against a set of realistic adult nasal airway replicas [19]. The plastic idealized geometry was able to mimic the *in vitro* regional deposition of nasal spray droplets averaged across a set of nine realistic nasal geometries in a single nasal spray (NasalCrom). However, due to the limitations of the plastic construction of the geometry, only water was suitable as a solvent for extracting deposited drug from geometry surfaces, and thus only one nasal spray product was tested. To test an expanded range of nasal drug delivery products and allow for the use of organic solvents in assaying, it was necessary to change the material of construction of the idealized geometry from plastic to metal. To that end, the Alberta Idealized Nasal Inlet (AINI; Copley Scientific, UK), an aluminum version of the idealized geometry described above, has been designed and manufactured.

The objective of the current study is to compare regional nasal deposition measurements made using the AINI with average *in vivo* regional deposition data across a range of nasal drug products.

Materials and Methods

Intranasal Drug Formulations

The choice of intranasal drug formulations for testing was motivated by two primary concerns. The first was to establish continuity of performance of the aluminum AINI with the version previously manufactured in plastic, and the second was to enable comparison of obtained *in vitro* regional deposition data with corresponding *in vivo* gamma scintigraphy data previously published in Al-Ghaneneem *et al.* (2008) and Leach *et al.* (2015) [19–21]. Accordingly, one aqueous solution formulation (cromolyn sodium; NasalCrom, Fisons Pharmaceuticals, Ipswich, UK), one aqueous suspension formulation (mometasone furoate; Nasonex, Merck & Co., Kenilworth, NJ, USA) and one nasal pMDI using HFA 134a as a propellant (beclomethasone dipropionate; QNASL, Teva Pharmaceutical Industries,

Tikva, Israel) were selected to encompass a range of devices and formulations.

Each Nasalcrom spray pump contains 13 mL of aqueous cromolyn sodium solution, with a label claim of 100 doses per spray pump (5.2 mg of cromolyn sodium per actuation). Nasonex spray pumps contain 120 doses of aqueous mometasone furoate suspension (50 µg per actuation). Finally, each QNASL spray device contains 120 doses of HFA-beclomethasone dipropionate formulation (80 µg per actuation).

Actuation Parameters

Each device was mechanically actuated by a Nasal Spray Products Universal Actuator (InnovaSystems Inc., Mooretown, New Jersey, USA). For the two nasal spray pumps (NasalCrom and Nasonex), force of actuation, force rise time, force hold time and force fall time were set according to mean *in vivo* values measured in adults previously reported by Doughty *et al.* (2010) and are shown in Table I. For QNASL, as is the case for pMDIs in general, it has been established that dosing is relatively insensitive to the aforementioned actuation parameters as long as the actuation force remains above a minimum threshold [22]. Insensitivity of the mass of the delivered dose with respect to actuation force in QNASL was confirmed in preliminary tests, with actuation forces ranging from 60 to 116 N. For deposition experiments, the actuation force for QNASL was set at 57.09 N (5.82 kg), which is well above the typical minimum force thresholds measured *in vivo* that are reported in the scientific literature [22–24].

Spray angle orientation (defined here as the angle the spray pump nozzle forms with the horizontal plane parallel to the lab bench surface) was chosen to correspond with the existing *in vitro* literature and to reflect patient use. Two angles, 60° and 45°, were selected both because of their high frequency of occurrence in a large number of *in vitro* nasal

Table I Actuation Parameters for Automated Repeatable Mechanic Actuation of the Nasal Spray Pump Obtained from Doughty et al. (2011) [24]. Each parameter is a Mean Value Averaged Across 20 Healthy Adults

Actuation force (kg)[a]	5.82
Rise time (ms)[b]	270
Release velocity (mm/s)[c]	34.87
Expected stroke length (mm)[d]	5.62

[a]Defined as the maximum force during the actuation

[b]Defined as the time required to reach the maximum force while actuating the pump

[c]Defined as velocity in releasing the pump

[d]Defined as the the maximum displacement of the pump during actuation

replica studies, and because these were the same angles used in our previous study validating the plastic idealized geometry [19, 25–29]. Since the nozzle of QNASL is angled 24° above the horizontal when the device is placed flat on the benchtop surface, compensatory adjustments in the mechanical actuator platform orientation were made. A steady inhalation flow rate of 7.5 L/min was chosen to mimic a slow nasal inhalation through a single nostril [19]. Each device required a different number of actuations into the AINI to ensure that quantifiable levels of the active ingredient could be collected for later UV–Vis spectroscopy: one actuation was used for NasalCrom, four actuations for Nasonex and two actuations for QNASL.

Experimental Procedure

A full description of the experimental procedure can be found in Chen *et al.* [19]. Briefly, each device was aligned according to the desired spray orientation angle, with the tip of the device raised until just penetrating the AINI inlet, and then actuated into the open inlet of the AINI. An antibacterial filter (ValuPlus! Viral/Bacterial Filter, KEGO Corporation, London, Ontario, Canada) was connected to the nasopharynx-side outlet of the AINI to capture any non-depositing particles escaping the AINI.

A schematic of the experimental setup is shown in Fig. 1. After actuation, a cotton wipe was held below the inlet to collect any formulation that may have dripped out of the Vestibule region of the AINI and to wipe benchtop and spray device surfaces after spraying. The AINI was then disassembled, and the filter, cotton wipe and each region were washed in an assay-appropriate solvent (water for Nasal-Crom; methanol for Nasonex and QNASL). The mass of formulation caught in the filter, collected by the wipe and deposited in each region of the AINI was then assayed using an ultraviolet–visible (UV–Vis) spectrophotometer (Cary 8454 UV—VIS System, Agilent Technologies, Santa Clara, California, USA).

In vitro Data Analysis

Data are presented as the relative fraction of the total dose entering the AINI that deposits on each of the nasal surfaces and in the filter. In other words, the deposition fraction in a specific region was calculated by dividing the mass of drug deposited on each region by the difference between total mass of drug recovered and the mass collected from dripping or wiped from the benchtop or external surfaces of the AINI.

To assess any impact of the construction material on regional deposition, deposition in the aluminum AINI was compared with deposition in the same idealized geometry previously manufactured in plastic as described in Chen *et al.* [19]. Thereafter, to facilitate comparison with available *in vivo* data from Leach *et al.* [21] and Al-Ghananeem *et al.* [20], separate regions of the AINI were combined when describing regional deposition. For Al-Ghananeem *et al.* [20], the *in vivo* anterior section corresponds to the AINI Vestibule, the *in vivo* posterior section corresponds to the combined AINI Turbinates and Olfactory regions and the pharynx region corresponds to the AINI Nasopharynx [20]. For Leach *et al.* [21], the Vestibule region of the AINI was assumed to correspond with the *in vivo* Nose region, the combined AINI Turbinates and Olfactory regions corresponded with the *in vivo* combined Mid and

Fig. 1 Schematic of experimental setup.
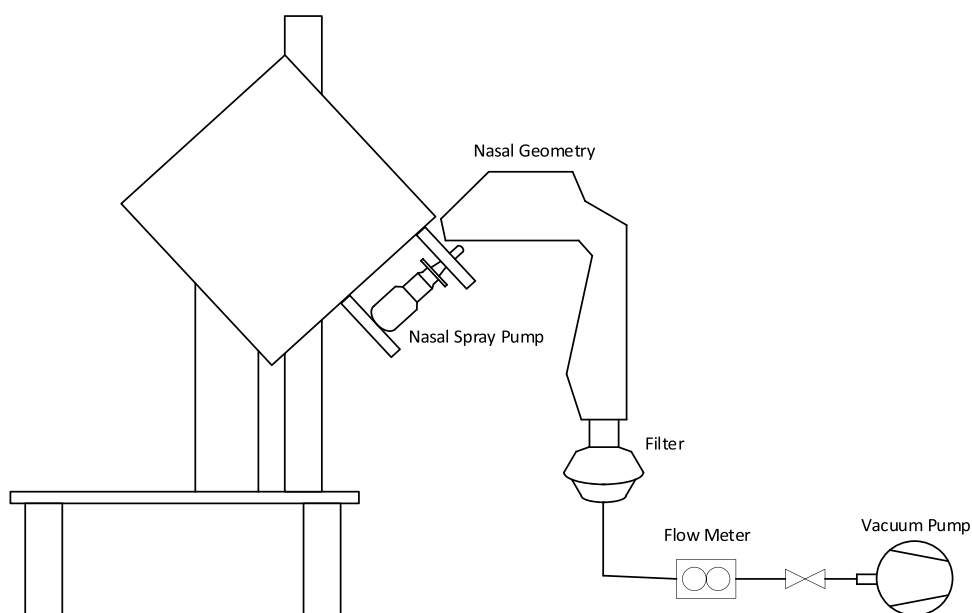
Upper nasal region, and the AINI Nasopharynx region corresponded with the *in vivo* Throat region [21].

Welch's *t*-test was used to detect differences in average regional deposition data owing to material of construction (plastic *vs*. metal) and spray angle orientation (60° *vs* 45°), with $P < 0.05$ considered significant, and was also used to compare *in vitro* data taken with the AINI with the *in vivo* gamma scintigraphy data. For the *in vitro-in vivo* comparison, *in vitro* deposition fractions at both orientations were pooled. Using the grouping schemes mentioned in the preceding paragraph, matching anatomical regions *in vitro* and *in vivo* were then statistically compared with gamma scintigraphy data from Al-Ghananeem *et al*. [20] or Leach *et al*. [21].

Results

In the present study, the fraction of the total delivered dose that dripped out of the Vestibule region ranged from 0 to approximately 0.5 (i.e. half) for the aqueous formulations. A substantial and variable amount of dripping was observed in every run of Nasonex, while only one instance of dripping was observed for NasalCrom. No dripping was detected for QNASL. Owing to the different number of actuations used in the *in vitro versus in vivo* studies, which may have contributed to the fraction of the total dose that would drip from the nose, the drip fraction was thus excluded when evaluating the ability of the AINI to mimic *in vivo* regional deposition.

No deposition was detected in either the Olfactory or Nasopharynx regions in any instance for all three chosen formulations. Thus, in several figures, deposition in the posterior section of the AINI refers solely to deposition in the Turbinates region, despite the posterior section technically including the Olfactory region as well. In addition, only for QNASL was there any deposition detected on the Filter fraction.

NasalCrom

Figure 2 shows comparisons of the regional deposition of NasalCrom in the metal AINI with previously published data taken using a plastic version of the same geometry and average *in vitro* regional deposition in a collection of realistic nasal airway replicas [19]. Figure 3 shows a comparison of the regional deposition profiles of NasalCrom in the AINI with *in vivo* deposition data published in Al-Ghananeem *et al*. [20]. The average total mass recovery from the AINI (including the wipe) was 98.8% with a standard deviation of 2.4%. Differences between regional deposition in the metal and plastic versions of the AINI were not statistically significant, indicating that the metal AINI is able to mimic *in*

vitro regional deposition in a set of realistic nasal airway replicas as closely as the previously validated plastic idealized geometry. *In vivo* deposition was also closely matched by the AINI, with deposition falling between the 45° and 60° extremes of the *in vitro* results.

Nasonex

Figure 4 shows a comparison of Nasonex regional deposition in the AINI at the 45° and the 60° orientations with available *in vivo* gamma scintigraphy data from Leach *et al*. [21]. The average total mass recovery (including the fraction collected by the wipe) in the AINI was 95.1% with a standard deviation of 15.1%. Deposition at 60° was higher in the Vestibule of the AINI than at 45°, but owing to the substantial run to run variance, this difference was not statistically significant.

QNASL

Figure 5 shows overall regional *in vitro* QNASL deposition in the AINI in terms of emitted dose, including the fraction which dripped from the vestibule after spraying. Figure 6 shows a comparison of the regional deposition of QNASL in the AINI at the 45° and 60° orientations with available *in vivo* data from Leach *et al*. [21]. The average *in vitro* total mass recovery was 88.0% with a standard deviation of 11.2%. Although Fig. 5 shows non-zero filter deposition, Fig. 6 deposition fractions have been normalized for total nasal delivery (i.e. total non-filter dose) to maintain consistency with the *in vivo* data. With or without normalization, the 60° orientation resulted in consistently high Vestibule deposition, but no statistically significant differences were observed between the two spray orientation angles. Overall, given the *in vitro* run-to-run variability, the AINI was generally able to mimic the *in vivo* regional deposition pattern.

Discussion

The objective of this study was to evaluate the *in vitro* performance of the AINI across a variety of nasal drug delivery products by comparing regional deposition profiles obtained from *in vitro* deposition experiments with corresponding profiles derived from previously published *in vivo* gamma scintigraphy data. No statistically significant differences were observed between *in viv*o and *in vitro* deposition in almost all cases, with the exception of Throat deposition for Nasonex ($P = 0.002$), which is unlikely to be clinically significant given the small deposition fraction (1.56%).

One broad trend that persisted across each of the three tested devices was the positive correlation between anterior deposition and the spray angle relative to the horizontal.

This trend agrees with both the general *in vitro* literature, which has in general reported higher anterior deposition with increasing orientation angle, and our previous publication utilizing the same geometry manufactured in plastic with NasalCrom as the test formulation [25, 26, 29–32].

As is evident from Figs. 2 and 3, regional deposition fractions measured for NasalCrom using the aluminum AINI agree with previously reported values obtained in a plastic version of the same geometry [19]. In addition, regional deposition fractions measured in the AINI matched average values previously measured across a set of realistic airway replicas at both angles of orientation, and were shown to

mimic available *in vivo* deposition data for NasalCrom (Fig. 3).

The other two formulations, Nasonex (a suspension) and QNASL (a propellant-based formulation), were chosen as additional test formulations to determine the ability of the AINI to mimic *in vivo* regional deposition patterns for a wider range of nasal preparations and devices. Leach *et al.* [21] is especially useful in this regard, not only because it gives a set of *in vivo* data from which to evaluate the performance of the AINI, but also because the usage of identical methodologies across two different devices was able to reveal large differences in the regional deposition
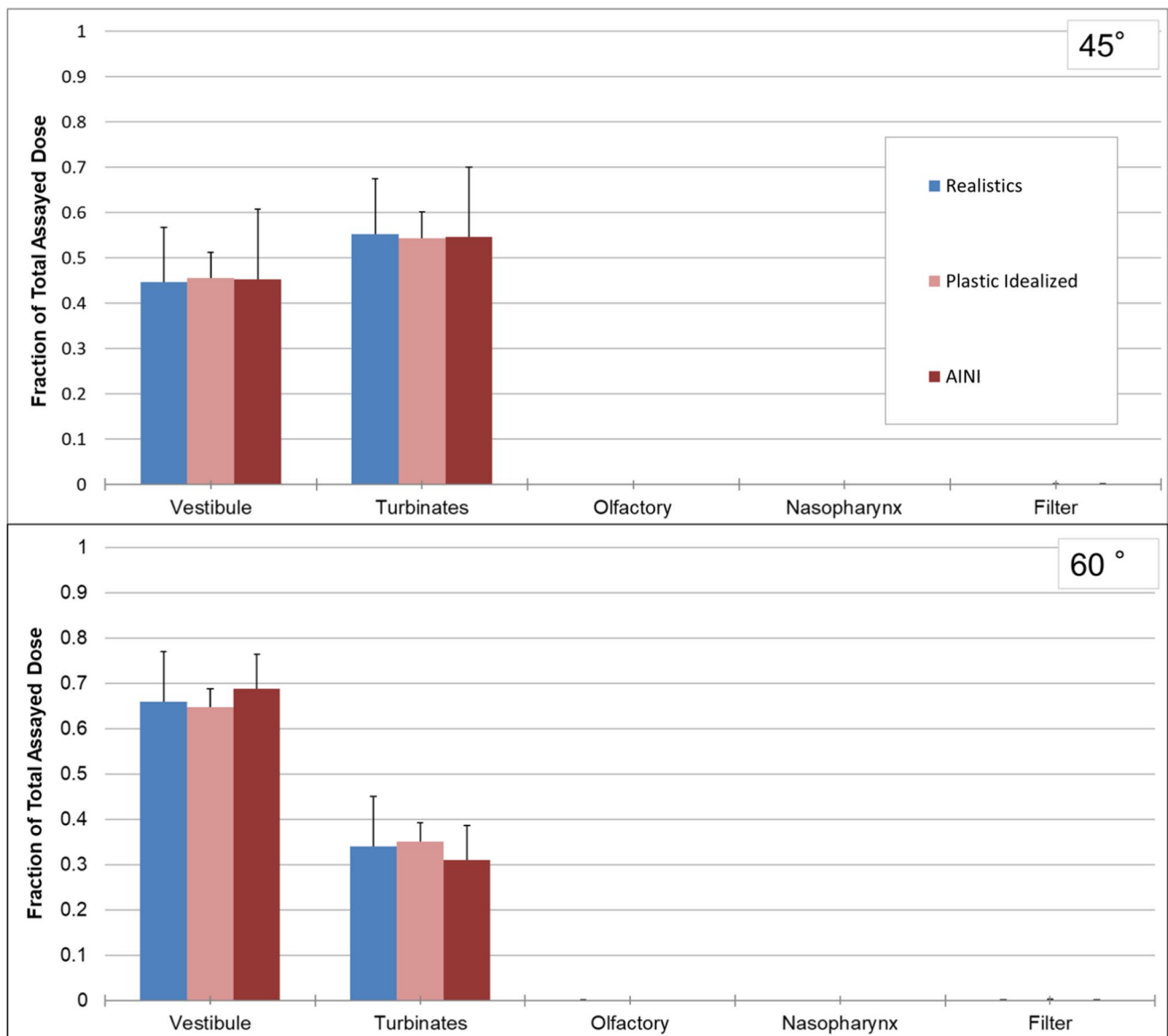

Fig. 2 Comparison of regional deposition of NasalCrom in realistic *vs.* idealized geometries (n = 3 repeats for plastic idealized, n = 3 repeats for AINI, n = 9 nostrils for realistics). Error bars indicate one standard deviation (measured across geometries for realistics and across repeats for idealized).
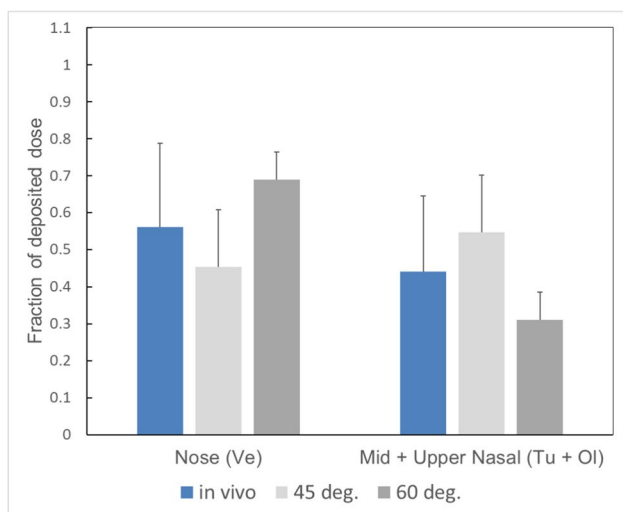
Fig. 3 Comparison of regional deposition of NasalCrom in AINI *vs. in vivo* (60° and 45°, n = 3 repeats for AINI, n = 9 nostrils for realistics). *In vivo* data taken from Al-Ghananeem *et al.* [20]. Note that administration angles *in vivo* were not reported. Error bars indicate one standard deviation (measured across repeats for AINI and across subjects for *in vivo*).

pattern between the aqueous (Nasonex) and propellant-based (QNASL) formulations [21]. Using this data, the ability of the AINI to replicate these differences can also be evaluated *in vitro*. Figure 4 shows that the AINI was able to predict *in vivo* deposition of Nasonex well when compared to Leach *et al.* [21], with *in vivo* deposition in both the anterior and posterior nose lying between the respective values measured
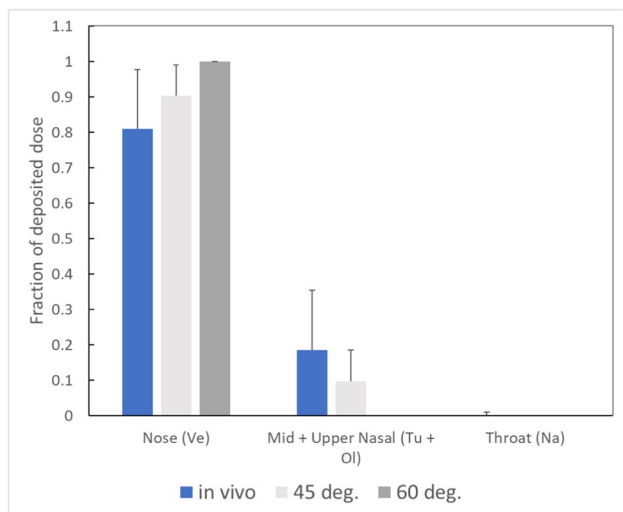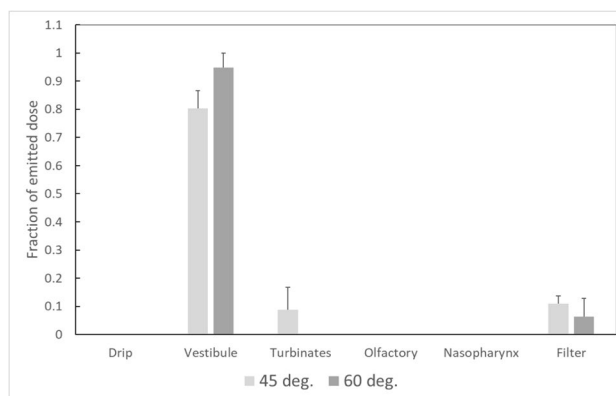

Fig. 5 Regional deposition of QNASL in AINI as fraction of emitted dose (i.e. including filter deposition and fraction dripping from the vestibule; 45° and 60°, n = 3 repeats for AINI). Error bars indicate one standard deviation (measured across repeats for AINI).

at the 60° and 45° orientations. In another *in vivo* gamma scintigraphy study with mometasone furoate, Shah *et al.* [33] measured posterior deposition beyond the nasal valve to be 60% of the delivered dose, contrary to previous *in vitro* and *in vivo* studies [33]. It is unknown if these differences in *in vivo* regional deposition represent real differences between the two small sample populations that were studied, or whether they are an artefact of methodological differences [34].

For QNASL, the *in vivo* data indicate that the bulk of deposition is concentrated strongly in the anterior region of the nose, a trend also reflected in the deposition pattern
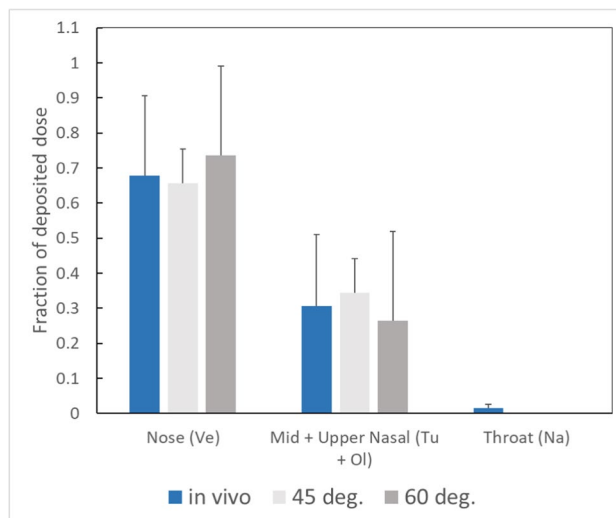

Fig. 6 Comparison of regional deposition of QNASL in AINI *vs. in vivo* data as fraction of dose deposited in the nasal cavity (i.e. excluding filter deposition; 45° and 60°, n = 3 repeats for AINI, n = 8 subjects for *in vivo*). *In vivo* data taken from Leach *et al.* [21]. Note that administration angles *in vivo* were not reported. Ve = Vestibule; Tu = Turbinates; Ol = Olfactory; Na = Nasopharynx. Error bars indicate one standard deviation (measured across repeats for AINI and across subjects for *in vivo*).

Fig. 4 Comparison of regional deposition of Nasonex in AINI *vs. in vivo* data as fraction of dose deposited in the nasal cavity (i.e. excluding filter deposition; 45° and 60°, n = 3 repeats for AINI, n = 9 subjects for *in vivo*). *In vivo* data taken from Leach *et al.* [21]. Note that administration angles *in vivo* were not reported. Ve = Vestibule; Tu = Turbinates; Ol = Olfactory; Na = Nasopharynx. Error bars indicate one standard deviation (measured across repeats for AINI and across subjects for *in vivo*).

observed in the AINI. Notable in the present *in vitro* data is the presence of a significant fraction of the delivered dose depositing on the filter, suggesting that a non-negligible portion of the dose is able to penetrate the nasal airways and possibly deposit in the lungs. Unfortunately, since lung deposition was not measured in Leach *et al.* [21], it is impossible to confirm *in vivo* penetration to the lungs [21]. However, *in vitro* deposition experiments done in a nasal airway replica in the Leach *et al.* study resulted in filter deposition of a magnitude similar to that found in the present study, which corroborates our findings and indicates the likely possibility of nonzero *in vivo* lung deposition [21].

Overall, notwithstanding factors such as the large variance *in vivo* and the differences in segmentation boundaries between the *in vivo* and *in vitro* cases that prevent an exact comparison, the AINI is able to predict average *in vivo* regional deposition.

This being said, the present study has limitations. The increased number of actuations (four) required for an accurate determination of Nasonex regional deposition using the UV–Vis assay does not reflect typical patient usage (one to two actuations per nostril) [21]. Moreover, the increased number of actuations led a large fraction of the deposited dose to drip from the AINI Vestibule, resulting in higher variability in regional deposition than would otherwise have been the case. This issue could potentially be avoided by utilizing a more sensitive assay, such as high-performance liquid chromatography or liquid chromatography–mass spectrometry.

However, the interior surfaces of the AINI have not been designed to mimic the surface wetting properties of a human nasal cavity. Thus, differences may exist between *in vitro* and *in vivo* measurements in the amount of formulation dripping from the nostril post-actuation, even for a lower number of actuations.

The lack of a precisely standardized segmentation scheme of the nasal cavity *in vitro* and *in vivo* has also likely contributed to some of the differences observed in the *in vitro* and *in vivo* deposition patterns. Moreover, because the segmentation scheme used for the AINI is fixed, the utility of the AINI may vary depending on the aims of the end user, especially if more granular distinctions between different anatomical regions of the nasal cavity are desirable in certain applications.

Finally, the AINI does not mimic dynamic changes of the nasal and oral airways throughout the breathing cycle. Thus, the AINI cannot be used to validate newer nasal drug delivery technologies that exploit such changes to improve delivery to the posterior nasal airways, for example by using the closure of the soft palate during exhalation to deliver smaller particle size drugs to the nasal cavity without risk of inhalation [35, 36].

Conclusions

The main objective of this study was to validate the ability of the AINI to mimic the average regional deposition pattern in a range of nasal drug delivery products. Benchtop *in vitro* experiments were designed and conducted using the AINI, and the resulting regional deposition patterns were compared to previously reported *in vitro* data and available *in vivo* data obtained using gamma scintigraphy. Good agreement was seen between regional deposition measured using the AINI and *in vivo* regional deposition patterns for all three nasal drug formulations that were tested. This suggests that *in vitro* testing incorporating the AINI may be useful in future intranasal drug delivery research and product development.

Declarations

References

1. Pharmacopiea U. Aerosols, nasal sprays, metered-dose inhalers, and dry powder inhalers. US Pharmacopeial [Internet]. 2006;30:2617–36. Available from: http://www.pharmacopeia.cn/v29240/usp29nf24s0_c601_viewall.html

2. U.S. Department of Health and Human Services, Food and Drug Administration Center for Drug Evaluation and Research D of DI (HFD-240). Draft: Guidance for Industry Bioavailability and Bioequivalence Studies for Nasal Aerosol and Nasal Sprays for Local Action. 2003; Available from: http://www.fda.gov/cder/guidance/index.htm

3. Newman SP, Pitcairn GR, Dalby RN. Drug Delivery to the Nasal Cavity: In Vitro and In Vivo Assessment. Critical Reviews in Therapeutic Drug Carrier Systems. 2004;21:46.

4. Li Bv, Jin F, Lee SL, Bai T, Chowdhury, Badrul Caramenico HT, Conner DP. Bioequivalence for locally acting nasal spray and nasal aerosol products: Standard development and generic approval. The AAPS Journal. 2013;15:875–83.

5. Below A, Bickmann D, Breitkreutz J. Assessing the performance of two dry powder inhalers in preschool children using an idealized pediatric upper airway model. International Journal of Pharmaceutics. Elsevier B.V.; 2013;444:169–74.

6. Javaherin E, Golshahi L, Finlaynn WH. An idealized geometry that mimics average infant nasal airway deposition. Journal of Aerosol Science Elsevier. 2013;55:137–48.

7. Delvadia RR, Longest PW, Byron PR. In vitro tests for aerosol deposition i: Scaling a physical model of the upper airways to predict drug deposition variation in normal humans. Journal of Aerosol Medicine and Pulmonary Drug Delivery. 2012;25:32–40.

8. Golshahi L, Finlay WH. An idealized child throat that mimics average pediatric oropharyngeal deposition. Aerosol Science and Technology. 2012;46.

9. Byron PR, Hindle M, Lange CF, Longest PW, McRobbie D, Oldham MJ, *et al*. In vivo-in vitro correlations: Predicting pulmonary drug deposition from pharmaceutical aerosols. Journal of Aerosol Medicine and Pulmonary Drug Delivery. 2010;23.

10. Ruzycki CA, Murphy B, Nathoo H, Finlay WH, Martin AR. Combined in Vitro-in Silico Approach to Predict Deposition and Pharmacokinetics of Budesonide Dry Powder Inhalers. Pharmaceutical Research. Pharmaceutical Research; 2020;37.

11. Ruzycki CA, Martin AR, Finlay WH. An Exploration of Factors Affecting in Vitro Deposition of Pharmaceutical Aerosols in the Alberta Idealized Throat. J Aerosol Med Pulm Drug Deliv. 2019;32:405–17.

12. Garcia GJM, Tewksbury EW, Wong BA, Kimbell JS. Interindividual Variability in Nasal Filtration as a Function of Nasal Cavity Geometry. Journal of Aerosol Medicine and Pulmonary Drug Delivery [Internet]. 2009;22:139–56. Available from: http://www.liebertpub.com/doi/https://doi.org/10.1089/jamp.2008.0713

13. Basu S, Holbrook LT, Kudlaty K, Fasanmade O, Wu J, Burke A, et al. Numerical evaluation of spray position for improved nasal drug delivery. Scientific Reports [Internet]. 2020;10:10568. Available from: http://www.nature.com/articles/s41598-020-66716-0

14. Foo MY, Sawant N, Overholtzer E, Donovan MD. A Simplified Geometric Model to Predict Nasal Spray Deposition in Children and Adults. AAPS PharmSciTech AAPS PharmSciTech. 2018;19:2767–77.

15. Pu Y, Goodey AP, Fang X, Jacob K. A comparison of the deposition patterns of different nasal spray formulations using a nasal cast. Aerosol Sci Technol. 2014;48:930–8.

16. Shah SA, Dickens CJ, Ward DJ, Banaszek AA, George C, Horodnik W. Design of Experiments to Optimize an In Vitro Cast to Predict Human Nasal Drug Deposition. J Aerosol Med Pulm Drug Deliv. 2013;27:21–9.

17. Schönbrodt T, et al. Method development for deposition studies in a nasal cast. In: Dalby RN, editor., et al., Respiratory Drug Delivery 2010. Orlando Florida: Davies Healthcare International Publishing; 2010. p. 445–9.

18. Darunkola MK. Simulation of Spray Deposition in Adults Nasal Airway. 2018.

19. Chen JZ, Kiaee M, Martin AR, Finlay WH. In vitro assessment of an idealized nose for nasal spray testing: Comparison with regional deposition in realistic nasal replicas. International Journal of Pharmaceutics [Internet]. Elsevier; 2020;582:119341. Available from: https://doi.org/10.1016/j.ijpharm.2020.119341

20. Al-Ghananeem AM, Sandefer EP, Doll WJ, Page RC, Chang Y, Digenis GA. Gamma scintigraphy for testing bioequivalence: A case study on two cromolyn sodium nasal spray preparations. Int J Pharm. 2008;357:70–6.

21. Leach CL, Kuehl PJ, Chand R, McDonald JD. Nasal Deposition of HFA-Beclomethasone, Aqueous Fluticasone Propionate and Aqueous Mometasone Furoate in Allergic Rhinitis Patients. J Aerosol Med Pulm Drug Deliv. 2015;28:334–40.

22. Ciciliani AM, Langguth P, Wachtel H. Handling forces for the use of different inhaler devices. International Journal of Pharmaceutics Elsevier. 2019;560:315–21.

23. Young PM, Price R. Comparative measurements of pressurised metered dose inhaler (pMDI) stem displacement. Drug Dev Ind Pharm. 2008;34:90–4.

24. Nakada H, Aomori T, Mochizuki M. Effect of a lever aid on hand strength required for using a handheld inhaler correctly. International Journal of Pharmaceutics. Elsevier B.V.; 2021;596:120249.

25. Foo MY, Cheng Y-S, Su W-C, Donovan MD. The Influence of Spray Properties on Intranasal Deposition. J Aerosol Med. 2007;20:495–508.

26. Hughes R, Watterson J, Dickens C, Ward D, Banaszek A. Development of a nasal cast model to test medicinal nasal devices. Proc Inst Mech Eng [H]. 2008;222:1013–22.

27. Inthavong K, Fung MC, Yang W, Tu J. Measurements of Droplet Size Distribution and Analysis of Nasal Spray Atomization from Different Actuation Pressure. J Aerosol Med Pulm Drug Deliv. 2014;28:59–67.

28. Kundoor V, Dalby RN. Effect of formulation- and administration-related variables on deposition pattern of nasal spray pumps evaluated using a nasal cast. Pharm Res. 2011;28:1895–904.

29. Warnken ZN, Smyth HDC, Davis DA, Weitman S, Williams RO, Kuhn JG. Personalized Medicine in Nasal Delivery: The Use of Patient-Specific Administration Parameters To Improve Nasal Drug Targeting Using 3D-Printed Nasal Replica Casts. Mol Pharm. 2018;15:1392–402.

30. Kundoor V, Dalby RN. Assessment of nasal spray deposition pattern in a silicone human nose model using a color-based method. Pharm Res. 2010;27:30–6.

31. Inthavong K, Tian ZF, Li HF, Tu J, Yang W, Xue CL, et al. A numerical study of spray particle deposition in a human nasal cavity. Aerosol Sci Technol. 2006;40:1034–45.

32. Xi J, Wang Z, Nevorski D, Zhou Y, Yuan JE, Zhang Y. Visualization and Quantification of Nasal and Olfactory Deposition in a Sectional Adult Nasal Airway Cast. Pharm Res. 2016;33:1527–41.

33. Shah SA, Berger RL, McDermott J, Gupta P, Monteith D, Connor A, et al. Regional deposition of mometasone furoate nasal spray suspension in humans. Allergy Asthma Proc. 2015;36:48–57.

34. Djupesland PG, Mahmoud RA. Letter to the editor: Incorrect conclusions regarding deposition of conventional mometasone furoate (MF) nasal spray. Allergy and Asthma Proceedings [Internet]. 2015;36:e104. Available from: http://www.ingentaconnect.com/content/https://doi.org/10.2500/aap.2015.36.3868

35. Djupesland PG. Nasal drug delivery devices: Characteristics and performance in a clinical perspective-a review. Drug Deliv Transl Res. 2013;3:42–62.

36. Kleven M, Melaaen MC, Reimers M, Røtnes JS, Aurdal L, Djupesland PG. Using Computational Fluid Dynamics (CFD) to Improve the Bi-Directional Nasal Drug Delivery Concept. Food and Bioproducts Processing [Internet]. 2005;83:107–17. Available from: https://linkinghub.elsevier.com/retrieve/pii/S0960308505704740